bioRxiv preprint doi: https://doi.org/10.1101/804864; this version posted October 16, 2019. The copyright holder for this preprint (which was not certified by peer review) is the author/funder, who has granted bioRxiv a license to display the preprint in perpetuity. It is made available under aCC-BY-NC-ND 4.0 International license.

Efficient and robust coding in heterogeneous recurrent networks

Fleur Zeldenrust[1,✉], **Boris Gutkin**[2,3], **and Sophie Denéve**[2]

[1]Department of Neurophysiology, Donders Institute for Brain, Cognition and Behaviour, Radboud University, Nijmegen, the Netherlands
[2]Group for Neural Theory, INSERM U960, Département d'Études Cognitives, École Normal Supérieure, Paris, France
[3]Department of Psychology, Center for Cognition and Decision Making, National Research University Higher School of Economics, Moscow, Russia

Cortical networks show a large heterogeneity of neuronal properties. However, traditional coding models have focused on homogeneous populations of excitatory and inhibitory neurons. Here, we analytically derive a class of recurrent networks of spiking neurons that close to optimally track a continuously varying input online, based on two assumptions: 1) every spike is decoded linearly and 2) the network aims to reduce the mean-squared error between the input and the estimate. From this we derive a class of predictive coding networks, that unifies encoding and decoding and in which we can investigate the difference between homogeneous networks and heterogeneous networks, in which each neurons represents different features and has different spike-generating properties. We find that in this framework, 'type 1' and 'type 2' neurons arise naturally and networks consisting of a heterogeneous population of different neuron types are both more efficient and more robust against correlated noise. We make two experimental predictions: 1) we predict that integrators show strong correlations with other integrators and resonators are correlated with resonators, whereas the correlations are much weaker between neurons with different coding properties and 2) that 'type 2' neurons are more coherent with the overall network activity than 'type 1' neurons.

Efficient coding | Filter networks | Recurrent networks | Type 1 and type 2 neurons | Trial-to-trial variability | Robustness against noise | Signal and noise correlations

Correspondence: ***f.zeldenrust@neurophysiology.nl***

Introduction

It is widely accepted that neurons do not form a homogeneous population, but that there is large variability between neurons. For instance, the intrinsic biophysical properties of neurons, such as the densities and properties of ionic channels, vary from neuron to neuron (1–5). Therefore, the way in which individual neurons respond to a stimulus (their 'encoding' properties or receptive field) also varies. A classical example is the difference between 'type 1' and 'type 2' neurons (6–10): 'type 1' neurons or 'integrators' respond with a low firing frequency to constant stimuli, which they increase with the amplitude of the stimulus. 'Type 2' neurons or 'resonators' on the other hand respond with an almost fixed firing frequency, and are sensitive to stimuli in a limited frequency band. Apart from these intrinsic 'encoding' properties of neurons, the 'decoding' propertes of neurons also show a large variability (see for instance (11)). Even if we do not take various forms of (short term) plasticity into account, there is a large heterogeneity in the shapes of post-synaptic potentials (PSPs) that converge onto a single neuron (for an overview: (12, 13)), depending on amongst others: the projection site (soma/dendrite: (14)), the number of receptors at the synapse, postsynaptic cell membrane properties ((15–17)), the type of neurotransmitter (GABAA, GABAB, glutamate), synapse properties (channel subunits, (18)), the local chloride reversal potential and active properties of dendrites (12). This heterogeneity results in variability of decay times, amplitudes and overall shapes of PSPs. So neural heterogeneity plays an important role both in encoding and in decoding stimuli. Whereas the study of homogeneous networks has provided us with invaluable insights (19–22), the effects of neural heterogeneity on neural coding have only been studied to a limited extent (23–25). Here we show that networks with spiking neurons with heterogeneous encoding and decoding properties can do optimal online stimulus representation. In this framework, neural variability is not a problem that needs to be solved, but it increases the networks' versatility of coding.

In order to investigate coding properties of neurons and networks, we need to use a framework in which we can assess the encoding and decoding properties and the network properteis. To characterize the relationship between neural stimuli and responses, filter networks (such as the Linear-Nonlinear Poisson (LNP) model (26), (27) and the Generalized Linear Model (GLM) (28, 29), for an overview, see (30), (31)) are widely used. In these models, each neuron in a network compares the input it receives with an 'input filter'. If the two are similar enough, a spike is fired. In a GLM, unlike the LNP model, this output spike train is filtered and fed back to the neuron, thereby incorporating effectively both the neuron's receptive field and history-dependent effects such as the refractory period and spike-frequency adaptation. It can be shown, that these types of filter-frameworks describe a maximum-likelihood relation between the input and the output spikes (32), (33). However, these models are purely descriptive: they only describe how spike trains are generated, not how they should be read out or 'decoded'. In this paper, we analytically derive a class of recurrent networks of spiking neurons that close to optimally track a continuously varying input online. We start with two very simple assumptions: 1) every spike is decoded linearly and 2) the network aims to perform optimal stimulus representation (i.e. reduces the mean-squared error between the input and the estimate). From this we derive a class of predictive coding networks, that unifies encoding

bioRxiv preprint doi: https://doi.org/10.1101/804864; this version posted October 16, 2019. The copyright holder for this preprint (which was not certified by peer review) is the author/funder, who has granted bioRxiv a license to display the preprint in perpetuity. It is made available under aCC-BY-NC-ND 4.0 International license.

(how a network represents its input in its output spike train) and decoding (how the input can be reconstructed from the output spike train) properties.

We investigate the difference between homogeneous networks, in which all neurons represent similar features in the input and have similar response properties, and heterogeneous networks, in which neurons represent different features and have different spike-generating properties. Firstly, we assess the properties of single-neuron (spike-triggered average, input-output frequency curve and phase-response curve) and show that in this framework, 'type 1' or 'integrator' (6, 34) neurons and resonators or 'type 2' neurons arise quite naturally. We show that the response properties of these neurons (the encoding properties, (35)) and dynamics of the PSPs they send (the decoding properties) are inherently linked, thereby giving a functional interpretation to these classical neuron types. Next, we investigate the effects of these different types of neurons on the network behaviour: we investigate the coding efficiency, robustness and trial-to-trial variability in *in-vivo*-like simulations. Finally, we predict that 1) integrators show strong correlations with other integrators and resonators are correlated with resonators, whereas the correlations are much weaker between neurons with different coding properties (36) and 2) that 'type 2' neurons are more coherent with the overall network activity than 'type 1' neurons

Methods

We analytically derive a recurrent network of spiking neurons that close to optimally tracks a continuously varying input online. We start with two assumptions: 1) every spike is decoded linearly and 2) the network aims to perform optimal stimulus representation (i.e. reduces the mean-squared error between the input and the estimate). We construct a cost function that consists of three terms: 1) the mean-squared error between the stimulus and the estimate, 2) a linear cost that punishes high firing rates and 3) a quadratic cost that promotes distributed firing. Every spike that is fired in the network reduces this cost function. The code for simulating such a network can be found at GitHub: github.com/fleurzeldenrust/Efficient-coding-in-a-spiking-predictive-coding-network.

Derivation of a filter-network that performs stimulus estimation. Suppose we have a set of N neurons j that use filters $g_j(t)$ to represent their input. Their spiking will give an estimated input equal to

$$\hat{s}(t) = \sum_{j=1}^{N} g_j(t) * \rho_j^{\text{ideal}}(t) = \sum_{j=1}^{N}\sum_{i=1}^{n_j} g_j(t-t_j^i), \quad \textbf{(1)}$$

where t_j^i are the spike times i of neuron j (what 'ideal' stands for will be explained later). The mean-squared error between the estimate $\hat{s}$ and the stimulus s equals

$$E(t) = \int_0^t (s(t)-\hat{s}(t))^2 dt = \int_0^t (s(t) - \sum_{j=1}^{N}\sum_{i=1}^{n_j} g_j(t-t_j^i))^2 dt. \quad \textbf{(2)}$$

Suppose that at time $t = T+\Delta$ we want to estimate the difference in error given that there was a spike of neuron m at time T or not. The difference in error is given by

$$\begin{aligned} &E^{\text{no spike at } T}(T+\Delta) - E^{\text{spike at } T}(T+\Delta) = \\ &\int_0^{T+\Delta} (s(t) - \sum_{j=1}^{N}\sum_{i=1}^{n_j} g_j(t-t_j^i))^2 dt \\ &- \int_0^{T+\Delta} (s(t) - \sum_{j=1}^{N}\sum_{i=1}^{n_j} g_j(t-t_j^i) - g_m(t-T))^2 dt = \\ &- \int_0^{T+\Delta} g_m(t-T)^2 dt \\ &+ 2\int_0^{T+\Delta} g_m(t-T)\left(s(t) - \sum_{j=1}^{N}\sum_{i=1}^{n_j} g_j(t-t_j^i)\right) dt. \end{aligned} \quad \textbf{(3)}$$

We introduce a greedy spike rule: a spike will only be placed at time T if this reduces the mean squared error at $T+\Delta$, so if the expression in equation (3) is positive. This results in a spike rule:

$$\begin{aligned} &\int_0^{T+\Delta} g_m(t-T)\left(s(t) - \sum_{j=1}^{N}\sum_{i=1}^{n_j} g_j(t-t_j^i)\right) dt \\ &\qquad > \frac{1}{2}\int_0^{T+\Delta} g_m(t-T)^2 dt. \end{aligned} \quad \textbf{(4)}$$

Obviously, if the decision is made at time $t = T+\Delta$, a spike cannot be placed in the past ($t = T$). Therefore, we introduce two spike trains: the real spike train $\rho(t)$, where a spike will be placed at time $T+\Delta$ with the spike rule above (equation (4)). This represents the 'ideal' spike train $\rho^{\text{ideal}}(t)$, which is $\rho(t)$ shifted by an amount of Δ, so that a spike at time $T+\Delta$ in $\rho(t)$ is equavalent to a spike at time T in spike train $\rho^{\text{ideal}}(t)$. This means that the neurons have to keep track of their own spiking history for at least Δ time and that any prediction of the input is delayed by an amount of Δ ($\sum_{j=1}^{N} g_j(t) * \rho_j(t)$ is an estimate of the input, delayed Δ in time).

Equation (4) defines a filter-network. Each neuron m keeps track of a 'membrane potential' V

$$\begin{aligned} V_m(T+\Delta) = &\int_0^{T+\Delta} g_m(t-T)s(t)dt \\ &- \int_0^{T+\Delta} g_m(t-T)\sum_{j=1}^{N}\sum_{i=1}^{n_j} g_j(t-t_j^i)dt, \end{aligned} \quad \textbf{(5)}$$

bioRxiv preprint doi: https://doi.org/10.1101/804864; this version posted October 16, 2019. The copyright holder for this preprint (which was not certified by peer review) is the author/funder, who has granted bioRxiv a license to display the preprint in perpetuity. It is made available under aCC-BY-NC-ND 4.0 International license.

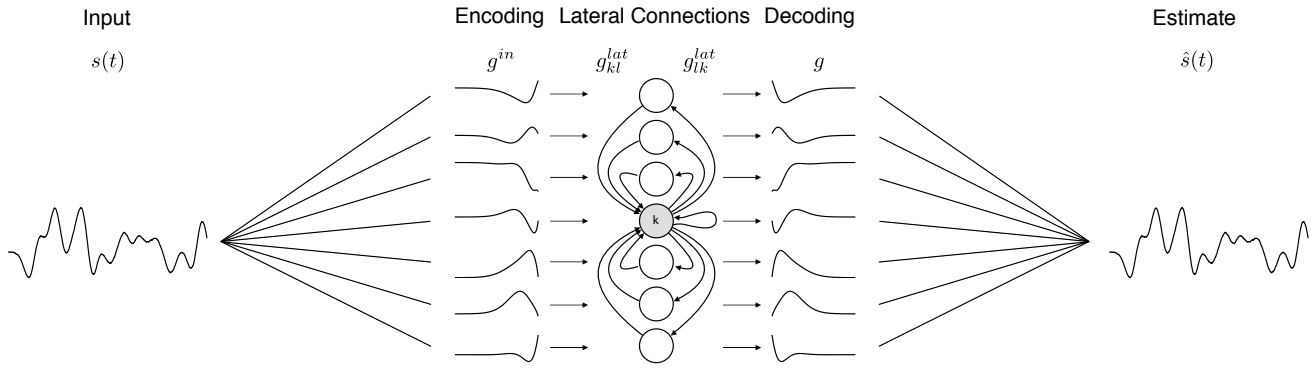

Fig. 1. Overview of the network model. Each neuron k filters the input $s(t)$ using an input filter g^{in}_k. It receives input from other neurons l via lateral filters g^{lat}_{kl} and sends input to other neurons l via lateral filters g^{lat}_{lk}. Finally, the network activity can be decoded linearly using decoding filters g_k.

that it compares to a threshold Θ

$$\Theta = \frac{1}{2}\int_0^{T+\Delta} g_m(t-T)^2 dt + \nu = \frac{1}{2}\int_{-T}^{\Delta} g_m(x)^2 dx, \quad \textbf{(6)}$$

Note that the threshold is not evaluated over the whole filter, but only between $t=-T$ and $t=\Delta$. Only if Δ is larger than the causal part of the filter and the proposed time of the spike T larger than the acausal part, the whole filter is taken into account, and the threshold reduces to $\Theta = \frac{1}{2}$ for (L2-norm) normalized filters.

The network defined by equation (4) can spike at any arbitrary frequency, and neurons show no spike-frequency adaptation. Two neurons that have identical filters except for their sign, have lateral filters $g^{\text{out}}_m(0) = 2(\Theta)$. Depending on the shape of the filter and the value of Δ, the maximum value of these lateral filters can exceed twice the threshold of the postsynaptic neuron, so a spike in a neuron can induce a spike in a neuron with a filter that is identical except for their sign. This 'ping-pong effect', which makes the estimate fluctuate very quicky around the ideal value, can be dampened by introducting a spike cost. So to force the network to choose solutions with realistic firing rates for each neuron, we introduce to additional terms to the threshold:

$$\Theta_c(t) = \frac{1}{2}\int_{-T}^{\Delta} g_m(x)^2 dx + \nu + \mu g^{\text{threshold}}(t-T), \quad \textbf{(7)}$$

where ν is a spike cost that punishes high firing rates in the network, which makes the code more sparse. $\mu g^{\text{threshold}}(t)$ is a spike cost kernel that punishes high firing rates in a single neuron (the effect is equivalent to spike-frequency adaptation) that makes the code more distributed between the neurons. In this paper we use an exponential kernel with time constant of 60 ms unless stated differently.

The first term on the right of equation (5) shows that neuron m is convolving the input $s(t)$ with an input filter $g^{\text{in}}_m(t)$ that is a flipped and shifted version of the filter neuron m represents:

$$\int_0^{T+\Delta} g_m(t-T)s(t)dt = \int_0^{T+\Delta} g^{\text{in}}_m(T+\Delta-t)s(t)dt = (g^{\text{in}}_m * s)(T+\Delta),$$

where

$$g^{\text{in}}_m(t) = g_m(\Delta - t). \quad \textbf{(8)}$$

Note that by introducing the time delay Δ between the evaluation time and the spike time, the input filter is now shifted relative to the representing filter. The representing filter can contain a causal part, that consists of the systems estimation on how the stimulus will behave in the near future of the spike, i.e. the systems estimation of the input auto-correlation. Any acausal part of the input filter is not used (since we do not know the future if the input $s(t)$), and vanishes as long as $g(t) = 0$ for $t > \Delta$. The optimal value of Δ depends on how much of a prediction the neuron wants to make into the future, but also on how long it is willing to wait with its response.

The second term of equation (5) denotes the lateral ($j \neq m$) and output ($j = m$) filters, that are substracted from the filtered input as a result of the spiking activity of any of the neurons. For well-behaved filters we can write

$$\begin{aligned}
&\int_0^{T+\Delta} g_m(t-T)\sum_{j=1}^{N}\sum_{i=1}^{n_j} g_j(t-t^i_j)dt \\
&= \sum_{j=1}^{N}\int_0^{T+\Delta} g_m(t-T)\left(g_j * \rho^{\text{ideal}}_j\right)(t)dt \qquad \textbf{(9)} \\
&= \sum_{j=1}^{N}\left(g^{\text{in}}_m * g_j * \rho^{\text{ideal}}_j\right)(T+\Delta),
\end{aligned}$$

so that we find an output filter

$$g^{\text{out}}_m(t) = -\left(g^{\text{in}}_m * g_m\right)(t) \quad \textbf{(10)}$$

and lateral filters

$$g^{\text{lat}}_{mj}(t) = -\left(g^{\text{in}}_m * g_j\right)(t), \quad \textbf{(11)}$$

bioRxiv preprint doi: https://doi.org/10.1101/804864; this version posted October 16, 2019. The copyright holder for this preprint (which was not certified by peer review) is the author/funder, who has granted bioRxiv a license to display the preprint in perpetuity. It is made available under aCC-BY-NC-ND 4.0 International license.

where t denotes the time since the spike of neuron j. Note that a spike at T can only influence the decision process at $T+\Delta$, so the part of the filter where $0 \leq t - t_j^i < t_j^i + \Delta$ does not influence the spiking process, and is therefore not used.

In summary, we defined network that can perform near-optimal stimulus estimation. Given a set of readout filters $g_i(t)$, the membrane potential of each neuron i is defined as

$$V_i(t) = g_i(t-\Delta) * \left(s(t) - \sum_{j=1}^{N} g_j(t) * \rho_j(t-\Delta) \right). \quad \textbf{(12)}$$

A spike is fired if this reduces the MSE of the estimate, which is equivalent to when the membrane potential exceeds the threshold Θ_c (equation (7)). This model has two main characteristics: the input, output and lateral filters are defined by the representing filter, and the representation of the input by the output spike train is delayed by an amount Δ in order for the network to use predictions for the stimulus after the spike.

We conclude that a classical filter network can perform near-optimal stimulus encoding given a certain relation between the input, output and lateral filters. In the classical framework of LNP and GLM models, acausal filters g are used, and the readout of the model is only used for information theoretic purposes. However, if the readout is being done by a next layer of neurons, one cannot use acausal filters: every spike of a presynaptic neuron m at time t_m^i, can only influence the membrane potential at its target at $t > t_m^i$ (i.e. can only cause a post-synaptic potential after the spike). Therefore, in a layered network, a self-consistent code will use only representative filters that are causal

$$g(t) = 0 \text{ if } t < 0$$

This means that for the input filters

$$g^{\text{in}} = 0 \text{ if } t > \Delta$$

Note that if $\Delta = 0$, the input filter reduces to a single value at $t = 0$. If $\Delta = 0$ and $g(0) = 0$, the input filter and hence the output and lateral filters vanish. Note that the threshold is scaled to the part of g between 0 and Δ, so not to the full integral over g. In this paper, we will normalize the input filters so that the thresholds are the same for all neurons.

Analysis.

Generation of neuron filters. In this paper, we choose each neuron filter on the basis of 8 basis functions given by the following Γ-functions:

$$\Gamma_n(t) = t^n e^{-t} \quad \textbf{(13)}$$

Type 1 neuron The representing filter of a 'type 1' neuron (figure 3 A & B, blue) is chosen equal to a Γ-function (equation (13)) with $n = 3$.

Type 2 neuron The representing filter of a 'type 2' neuron (figure 3 A & B, red) is chosen as $g_{\text{type 2}}(t) = \Gamma_3(t)(0.2 - 0.8\sin(0.6t))$.

Off cells We call a neuron with an inverted representing filter an 'off cell'. So a 'type 1 off cell' has representing filter $g_{\text{type 1, off}}(t) = -\Gamma_3(t)$ and a 'type 2 off cell' has representing filter $g_{\text{type 2, off}}(t) = -\Gamma_3(t)(0.2 - 0.8\sin(0.6t))$

Homogeneous network The representing filters of a 'type 1'-network are equal to the 'type 1' neuron (half of the neurons) or minus the 'type 1' neuron (other half of the neurons).

Type 1 & type 2 network A quarter of the representing filters of the neurons in the network are equal to the 'type 1' neuron, a quarter to minus the 'type 1' neuron, a quarter to the 'type 2' neuron and a quarter to minus the 'type 2' neuron.

Heterogenous network The representing filters in the heterogenous network are products of Γ functions and oscillations. This is in order to ensure that they have realistic properties (i.e. vanishing after tens of milisecondes), while still being able to represent different frequencies. Half of the neurons have a representing filter equal to $g_n(t) = \Gamma_3(t)(0.2 \pm 0.8\sin(\psi t))$, with ψ a random number between 0 and 1.5 and half of these using an addition and half a subtraction. The representing filters of the other half of the population are given by $g_n(t) = \Gamma_3(t)(0.2 \pm 0.8\cos(\psi t))$.

Spike Coincidence Factor. The coincidence factor Γ (37, 38) describes how similar two spike trains $s_1(t)$ and $s_2(t)$ are: it reaches the value 1 for identical spike trains, vanishes for Poissonian spike trains and negative values hint at anti-correlations. It is based on the binning of the spike train in $K = \frac{T}{p}$ bins of binwidth p. The coincidence factor is corrected for the expected amount of coincidences $\langle N_{\text{coinc}} \rangle$ of spike train s_1 with a Poissonian spike-train with the same rate ν_2 as spike train s_2. It gives a measure of 1 for identical spike trains, 0 if all coincidences are accidental and negative values for anti-correlated spike trains. It is defined as

$$\Gamma_{12} = \frac{N_{\text{coinc}} - \langle N_{\text{coinc}} \rangle}{\frac{1}{2}(N_1 + N_2)} \frac{1}{\mathbb{N}} \quad \textbf{(14)}$$

in which

$$\langle N_{\text{coinc}} \rangle = 2\nu_2 p N_1 = \frac{2N_1 N_2}{K}$$

Finally, Γ is normalized by

$$\mathbb{N} = 1 - 2\nu_2 p = 1 - \frac{N_2}{K}$$

so it is bounded by 1. Note that the coincidence factor is not symmetric nor positive, therefore it is not a metric. It is only defined as long as each bin contains at most one event, however, we counted the bins with double spikes as bins containing one spike. Finally, it will in general saturate at a value

bioRxiv preprint doi: https://doi.org/10.1101/804864; this version posted October 16, 2019. The copyright holder for this preprint (which was not certified by peer review) is the author/funder, who has granted bioRxiv a license to display the preprint in perpetuity. It is made available under aCC-BY-NC-ND 4.0 International license.

below one, which can be seen as the reliability. The rate as which it reaches this value (for instance as defined by a fit to an exponential function) can be seen as the precision. In section we calculated the coincidence factor between the spike-train response to each stimulus presentation for each neuron in the network, and averaged this over neurons to obtain a $\overline{\Gamma}$, a measure for the trial-to-trial variability or the degeneracy of the code of the network (figure 4, left).

Mean-Squared Error, Network Activity and Effciency. The Mean-Squared Error (MSE) is for N measurements in time is defined by

$$MSE(s, \hat{s}) = \sum_{n=1}^{N} (s_n - \hat{s}_n)^2$$

However, this typically increases with the stimulus amplitude and length. To assess the performace of networks independently of stimulus amplitude, we normalized the mean-squared error by deviding it by the mean-squared error between the stimulus and an estimate of a constant zero signal (or equivalently, the MSE between the stimulus and network estimate if the network would be quiescent, $\text{MSE}_{\text{no spikes}}$):

$$\overline{\text{MSE}} = \frac{\text{MSE}}{\text{MSE}_{\text{no spikes}}}. \tag{15}$$

An $\overline{\text{MSE}}$ close to zero means a good performance, whereas a value close to one means performance that is comparable to a network that doesn't show any activity. Given that the goal of this network is to give an approximation of the input signal with the lowest number of spikes as possible, we define the network activity A (in Hz) as

$$A = \frac{\#\text{ spikes}}{N_{\text{neuron}} T_{\text{sim}}}, \tag{16}$$

where N is the number of neurons, and T the duration of the stimulus, and the efficiency E (in seconds) of the network as

$$E = \frac{1}{\overline{\text{MSE}} \cdot A}. \tag{17}$$

Results

In this section, we will discuss the properties of the network derived in section . We will start with the general network behaviour, and show that it can track several inputs. Next, we will show that this framework provides a functional interpretation of 'type 1' and 'type 2' neurons. In the following sections, we will zoom in on the relation between trial-to-trial variability and the degeneracy of the code used, and on the network's robustness to noise. Finally, we will make experimental predictions based on the network properties.

Network response. In figure 2, the response of two different networks is shown: a homogeneous network, consisting of 50 neurons with a positive representing filter g (see section) and 50 neurons with a negative one and a heterogeneous network (bottom), consisting of 100 neurons with each a different (but normalized, based on Γ-fuctions) representing filter g. Both networks can track both constant and fluctuating inputs with different frequencies well. Note that even though there is no noise in the network, the network response is quite irregular, like in *in-vivo* recordings. Note also that the heterogeneous network is better at tracking fast fluctuations. How well the different types of networks respond to different types of input, what the response properties of the networks are, and what the influence of the type of filter g is, will be investigated in the following sections.

'Type 1' and 'type 2' neurons. If we create representing filters randomly (see section), they generally fall into one of two types: unimodal ones (only postitive or only negative) or bimodal ones (both a positive and a negative part). In this section, we will investigate the difference between neurons using these two types of representing filters.

In figure 3 the response of a single neuron with a unimodal (blue) or multimodal (red) representing filter (both are normalized with respect to the input filter g_{in}, so between $t = 0$ ms and $t = \Delta = 7,5$ ms) to different types of input is shown (see section). Note that these simulations are for single neurons, so there is no network present, like in *in-vitro* patch-clamp experiments. A neuron with a unimodal representing filter (figure 3 A and B, blue) shows a continuous input-frequency curve (figure 3 C and D). Such a neuron with a unimodal representing filter has a unimodal Phase Response Curve (PRC) and Spike-Triggered Average (STA) (figure 3 E and F). A neuron with a multimodal representing filter (figure 3 A and B, red) does initially only respond with a single spike to the switching on of the step-and-hold current. Only for high current amplitudes it starts firing pairs of doublets, due to the interaction between the filtering properties and the spike-frequency adaptation. It has a bimodal PRC within the doublets (figure 3 E, solid red line), but a unimodal PRC between the doublets (figure 3 E, dashed red line) . Such a neuron with a multimodal representing filter also has a bimodal Spike-Triggered Average (figure 3 F, red line). The input-frequency curves, PRC and STA together, show that neurons with unimodal representing filters show 'type-1' -like behaviour, whereas neurons with multimodal fitlers show 'type 2'-like behaviour.

Homogeneous and heterogeneous networks. In the previous section, we showed that 'type 1' and 'type 2' neurons appear naturally in the predictive coding framework we defined in section . Even though the single-neuron response properties of 'type 1' and 'type 2' neurons have been studied extensively, most simulated network consist of a single or a few homogeneous populations of leaky integrate-and-fire ('type 1') neurons. Here, we will investigate the effect of heterogeneity in the response properties of single neurons on the network properties and dynamics. We will compare a homogeneous network consisting of 'type 1'-neurons, an intermediate network consisting of 'type 1' and 'type 2'-neurons, and a heterogeneous network (see section).

bioRxiv preprint doi: https://doi.org/10.1101/804864; this version posted October 16, 2019. The copyright holder for this preprint (which was not certified by peer review) is the author/funder, who has granted bioRxiv a license to display the preprint in perpetuity. It is made available under aCC-BY-NC-ND 4.0 International license.

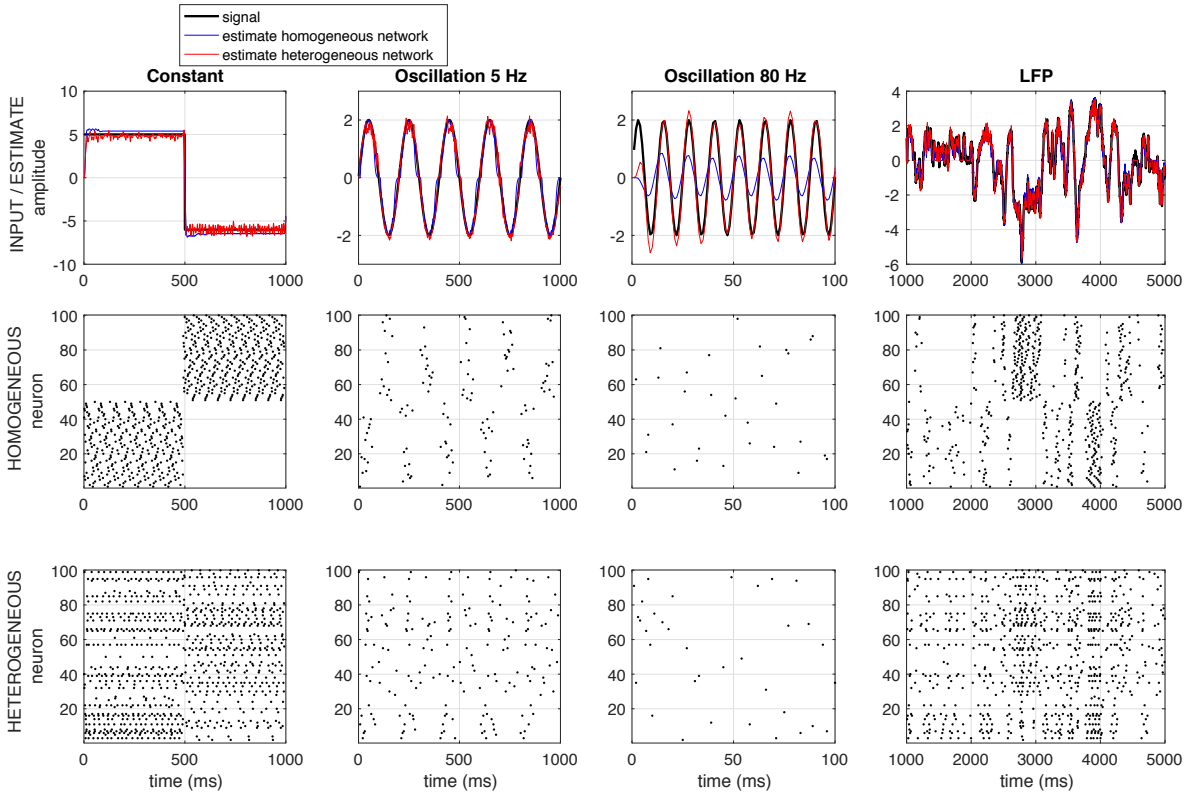

Fig. 2. Example of the response of a homogeneous (red) and a heterogeneous (blue) network to a constant input (first column), to a low frequency input (5 Hz, second colum), to a high frequency input (80 Hz, third column) and to a recorded LFP-signal (right). The homogeneous network consists of 50 neurons with a positive representing filter g and 50 neurons with a negative one (see section); the heterogeneous network consists of 100 neurons with each a different (but normalized) representing filter g. Network parameters: $\Delta = 7,5$ ms, $\nu = \mu = 0.5$. No noise is added to this network.

Heterogeneous networks are more efficient than homogeneous networks. The trial-to-trial variability of network responses depends critically on both the network structure and on the input stimuli used. For instance, it has been shown that (sub)cortical responses to stimuli with naturalistic statistics are more reliable than responses to other stimuli(39–45). This suggests that, depending on the cortical area and the input statistics, neural networks can use codes that are highly degenerate or non-degenerate. For clarification, we define here a degenerate code as a code in which the stimulus can be represented with a low error by several different population responses. Therefore, a degenerate code will show a high trial-to-trial variability, or a low reliability. We hypothesize that a network consisting of neurons that represent similar features of the common input signal (i.e. several neurons have the same representing filter g) will use more degenerate codes than networks consisting of neurons that represent different features of the input signal (i.e. every neuron has a different representing filter g). So we hypothesize that homogeneous networks will show a higher trial-to-trial variability (i.e. a lower reliability). Here, we investigate the relation between trial-to-trial variability, network performance, input statistics and the network heterogeneity. We do this by simulating the response of three different networks with increasing levels of heterogeneity (a network consisting only of identical 'type 1' neurons, a mixed network consisting of 'type 1' and 'type 2' neurons and a heterogeneous network in which each neuron is different, see section) to input stimuli with different statistical properties (varying the amplitude and the autocorrelation time constant τ).

In figure 4, we simulated three networks (see also section): a homogeneous network (first row), a mixed network (second row, consisting for 50 % of 'type 1' neurons (positive and negative filters) and for 50 % of 'type 2' neurons (positive and negative filters) and a heterogeneous network (third row). We varied both the amplitude and the time constant of the input signal (by filtering the input forwards and backwards with an exponential filter). To determine the level of degeneracy of the code the network uses, we performed the following simulations: we computed the network response to the same stimulus ($T = 2500$ ms) twice, but before this stimulus started, we gave the network a 500 ms random start-stimulus. Note that there was no noise in the network except for the different start-stimuli. We calculated four network performance measures:

Network Activity A (Hz) We assessed the total network activity (figure 4, first column), as the average firing frequency per neuron (see section).

Reliability Γ The coincidence factor Γ (37, 38) (see section) describes how similar two spike trains are: it reaches a value of 1 for identical spike trains, vanishes for Poisson spike trains and negative values hint at anti-

bioRxiv preprint doi: https://doi.org/10.1101/804864; this version posted October 16, 2019. The copyright holder for this preprint (which was not certified by peer review) is the author/funder, who has granted bioRxiv a license to display the preprint in perpetuity. It is made available under aCC-BY-NC-ND 4.0 International license.

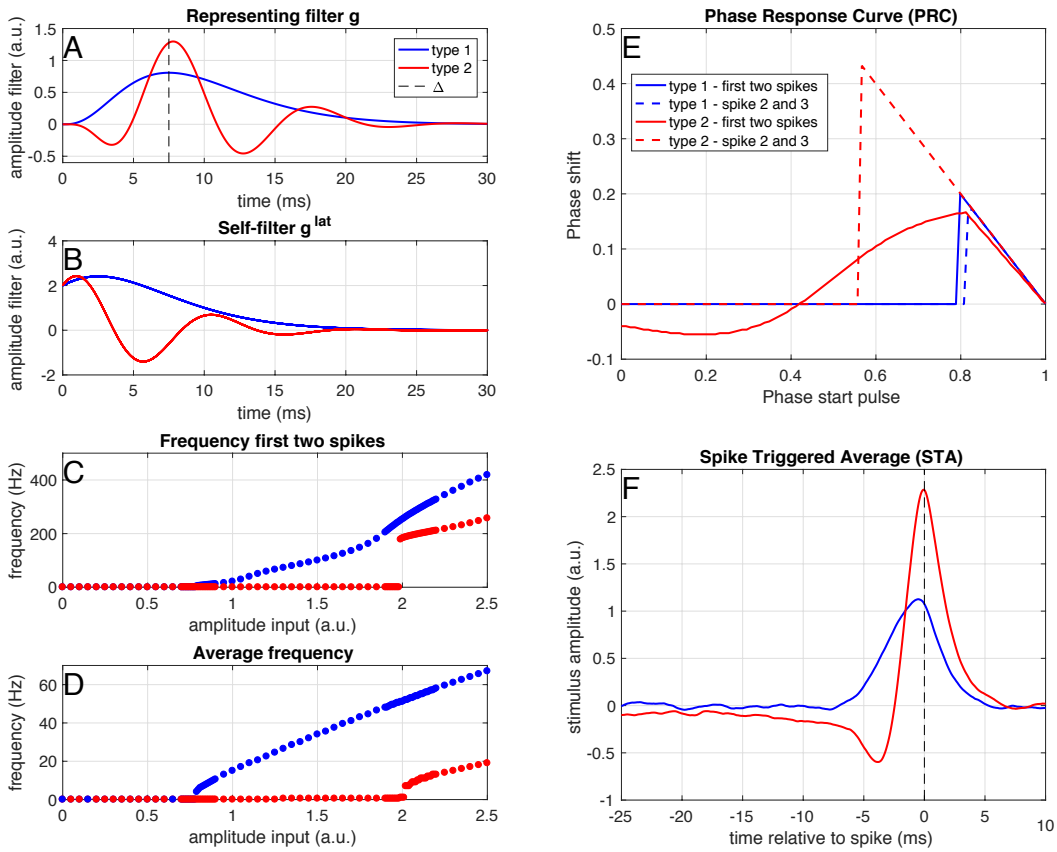

Fig. 3. Example of a 'type 1' (blue) and a 'type 2' (red) neuron. A) Representing filter of a 'type 1' (blue) and a 'type 2' (red) neuron. B) Self-filters for both neuron types. C) Instantaneous frequency of the first two spikes in response to step-and-hold inputs of different amplitudes. D) Average frequency in response to step-and-hold inputs of different amplitudes. E) Phase-response curves for the first and second pairs of spikes, calculated as response to a small pulse (0.1 ms, amplitude 1.5 ('type 2') and 3.7 ('type 2')) on top of a constant input (amplitude 0.9 ('type 1') and 2.2 ('type 2')). F) Spike-triggered average in response to a white-noise stimulus (amplitude: 0.45 ('type 1') and 1.1 ('type 2')) filtered with an exponential filter with a time constant of 1 ms.

correlations. We calculated the coincidence factor between the spike-train response to each stimulus presentation for each neuron in the network, and averaged this over neurons to obtain $\overline{\Gamma}$, a measure for the trial-to-trial variability of the network (figure 4, second column). If the network uses a highly degenerate code, the starting stimulus will put it in a different state just before the start of the stimulus used for comparison, and the trial-to-trial variability will be high (low $\overline{\Gamma}$). On the other hand, if the network uses a non-degenerate code, the starting stimulus will have no effect, and the trial-to-trial variability will be low (high $\overline{\Gamma}$). Therefore, $\overline{\Gamma}$ (figure 4, left) represents the non-degeneracy of the code: a $\overline{\Gamma}$ close to zero corresponds to a high degeneracy and a high trial-to-trial variability, and a $\overline{\Gamma}$ close to one a low degeneracy and a low trial-to-trial variability.

Error $\overline{\text{MSE}}$ To assess the performace of the network, we calculated the normalized mean-squared error ($\overline{\text{MSE}}$ (figure 4, third column), see section), so that a value of $\overline{\text{MSE}}$ close to zero means a good network performance, and a value close to one means performance that is comparable to a network that doesn't show any activity.

Efficiency E (s) Given that the goal of this network is to give an approximation of the input signal with the lowest number of spikes as possible, we define the network efficiency (in seconds) as the inverse of the product of firing rate and the error (see section), so that the efficiency decreases with both the network activity and the error ($\overline{\text{MSE}}$ (figure 4, fourth column).

In figure 4, it is shown that all three networks (homogeneous, type 1 & type 2 and heterogeneous, respective rows) perform well (small error, second column) over a wide range of stimulus amplitudes and frequencies. The performance of the network depends strongly on the heterogeneity of the network and the characteristics of the stimulus: heterogeneous networks show a smaller $\overline{\text{MSE}}$ (second column), especially for fast-fluctuating (small τ) input. However, this comes at the cost of a higher activity A (first column), in particular at larger stimulus amplitudes. If we summarize this by the efficiency E (fourth column), we see that the heterogeneous network is more efficient, in particular for low amplitude and fast fluctuating stimuli.

The amplitude of the stimulus relative to the amplitudes of the neural filters and the amount of neurons is important: to represent a high-amplitude stimulus requires all the neurons to fire at the same time, which makes the code highly

bioRxiv preprint doi: https://doi.org/10.1101/804864; this version posted October 16, 2019. The copyright holder for this preprint (which was not certified by peer review) is the author/funder, who has granted bioRxiv a license to display the preprint in perpetuity. It is made available under aCC-BY-NC-ND 4.0 International license.

non-degenerate: Since the filter amplitudes are between 1 and 2, a stimulus with an amplitude (standard deviation) of 20 would need an equivalent number of the $N = 100$ neurons (the ones with a positive filter) to spike at the same time to reach the amplitude of the peaks. This results in a reliable, non-degenerate code (high $\overline{\Gamma}$). Alternatively, when a low-amplitude stimulus is represented by many neurons with relatively high-amplitude filters, the network can 'choose' which neuron to use for representing the input, thereby making the code degenerate (low $\overline{\Gamma}$). [1]. This is reflected in the reliability $\overline{\Gamma}$ (third column). In a homogeneous network consisting of identical neurons representing a low amplitude input, there is no difference between a spike of neuron A or one of neuron B, making the code highly degenerate (low $\overline{\Gamma}$). When the amplitude of the stimulus increases, more neurons are recruited to represent the stimulus, thereby increasing both the network activity A and the reliability $\overline{\Gamma}$. When the stimulus amplitude becomes too high to represent properly, both the error $\overline{\text{MSE}}$ and $\overline{\Gamma}$ increase sharply (bottom left), and the efficiency E decreases (bottom right). Therefore, a high trial-to-trial variability, or a low reliability $\overline{\Gamma}$ is a hallmark of an efficiently coding network, and a strong decrease of the trial-to-trial variability (an increase in $\overline{\Gamma}$) is a sign of a network starting to fail to track the stimulus. This happens for lower amplitudes for the heterogeneous network than for the homogeneous network.

In conclusion, all three networks can track stimuli with a wide range of parameters well, but the heterogeneous network performs shows a lower error for an only small increase in activity, therefore the heterogeneous network is more efficient than the homogeneous network. However, the homogeneous network can track higher amplitude stimuli, in particular slowly fluctuating ones. The efficiency of the code shows a strong inverse relation with the trial-to-trial variability: the higher the network reliability, the lower its efficiency. So a high trial-to-trial variability is a hallmark for an efficiently coding network.

Heterogeneous networks are more robust against correlated noise than homogeneous networks. In the previous section it was shown that heterogeneous networks are more efficient than homogeneous networks in encoding a wide variety of stimuli. However, these networks did not contain any noise. It has been shown that cortical networks receive quite noisy input, which is believed to be correlated between neurons(46–48). Therefore, we will test in this section how robust homogeneous and heterogeneous networks are against correlated noise.

To test for robustness against noise, we chose a stimulus that all networks responded well to: amplitude $= 10$, $\tau = 15$ ms (see the white start in figure 4). Noise was added in a 'worse case scenario': it had the same temporal properties as the stimulus (i.e. it was white noise filtered with the same filter with $\tau = 15$ ms) and several neurons received the same noise. Two parameters were varied: the amplitude of the noise, and the correlations between the noise signals that different neurons receive. This was implemented as follows: next to the stimulus, every neuron received a noise signal and we varied the relative amplitude of the noise signal ($a_{\text{noise}}/a_{signal}$). Correlations between the noise signals for different neurons were simulated by only making a limited amount of noise copies, that were distributed among the neurons. So in figure 5, the top horizontal row of each axis corresponds to the situation in which each neuron receives an independent noise signal, the bottom horizontal row of each axis represents the situation where all neurons receive the same noise signal (and hence there is from the network's point of view no difference between signal and noise). So in figure 5, the leftmost column of each axis corresponds to the situation without noise, the top row corresponds to a simulation where all neurons in the network recieve an independent noise signal and the bottom row corresponds to the situation where every neuron receives the same noise signal.

In figure 5, it is shown that all three networks are very effective in compensating for independent noise by increasing their firing rate. Note that the stimulus and the noise add quadratically, so that a signal with amplitude 10 and noise with amplitude 12 (relative amplitude 1.2) add together to a total input of amplitude $\sqrt{10^2 + 12^2} = 15.5$ for each neuron. However, the firing rate of a network with signal amplitude = 10 and noise amplitude = 12, is much higher than the firing rate of a network that receives a signal with amplitude 15.5 and no noise (compare figures 4 and 5). So the networks increase their activity both due to the increased amplitude of the input, and in order to compensate for noise. The top row of each subplot in figure 5 corresponds to a simulation where all neurons in the network recieve the same noise signal. In this case, it is impossible for the network to distinguish between signal and noise. In the row above, only two noise copies are present, in the row above that five, and so on. The homogeneneous network can handle higher amplitudes of independent noise (top part of each subplot) before the representation breaks down ($\overline{\text{MSE}} > .2$), but all networks are able to compensate for independent noise amplitudes up to equal to the signal amplitude (signal-to-noise ratio = 1). The heterogeneous network however, is better at dealing with correlated noise (bottom part of each subplot): it shows a lower error and higher efficiency for when there are few copies of the noise signal. The type 1'& type 2 network appears to combine the properties of both networks: it has a low error in both representing independent noise and at representing correlated noise. These differences in robustness against noise probably have a relation with ambiguities in degenerate codes, as will be discussed in section .

Experimental predictions. In the previous sections, we derived a predictive coding framework and assessed the efficiency and robustness of representing a stimulus of homogeneous and heterogeneous networks. In this section, we will

[1] However, note that none of the networks are very good at responding to very low stimulus amplitudes: this is because most fluctuations are smaller than the filter amplitudes

bioRxiv preprint doi: https://doi.org/10.1101/804864; this version posted October 16, 2019. The copyright holder for this preprint (which was not certified by peer review) is the author/funder, who has granted bioRxiv a license to display the preprint in perpetuity. It is made available under aCC-BY-NC-ND 4.0 International license.

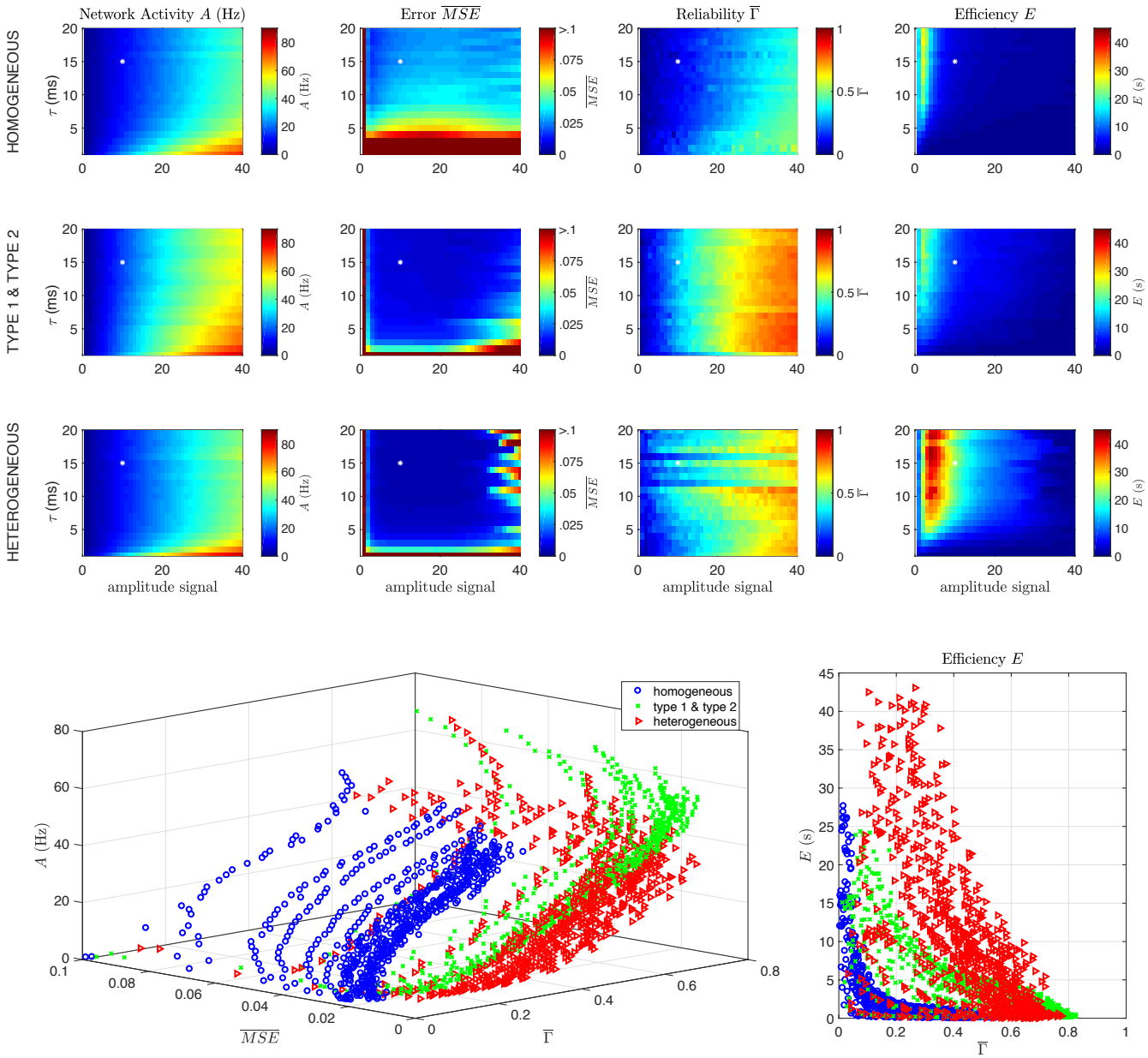

Fig. 4. Heterogeneous networks are more efficient and show less trial-to-trial variability. Results of two simulations using the same stimulus, but different initial network states, in a homogeneous 'type 1' network (first row), a network with 'type 1' and 'type 2' neurons (second row) and a heterogeneous network (third row). The network network activity A (first column), reliability $\overline{\Gamma}$ (second column), network $\overline{\text{MSE}}$ (third column) and efficiency E (fourth column) are shown as a function of the time constant (τ) and amplitude of the stimulus. All networks perform well over a wide range of stimulus amplitudes and frequencies, but the heterogeneous network is more efficient for a wider range of input parameters, in particular for fast-fluctuating low amplitue signals. The bottom row shows how the network activity, error and efficiency depend on the reliability $\overline{\Gamma}$. Parameters: $\Delta = 7,5$ ms, $\nu = \mu = 1,5$, $N = 100$. The white star denotes the parameter values used in section

include experimental predictions with respect to the predictive coding framework and the effect it has on correlation structures.

Signal and noise correlations. The predictive coding framework that we derived in section predicts a specific correlation structure: neurons with similar filters g should show positive signal correlations (because they use similar input filters), but negative noise (also termed spike count) correlations (because they have negative lateral connections). In many experimental papers, noise and signal correlations between neurons are measured (49, 50) (for an overview, see (51)). However, the methods authors use vary strongly: the amount of repetitions of the stimulus varies from tens to hundreds, the windows over which correlations are summed vary from tens of miliseconds to hundreds of miliseconds and the strength of the stimulus (i.e. network response) varies from a few to tens of Hz. All these parameters strongly influence the conclusions one can draw about correlations between (cortical) neurons. In order to be able to compare the correlations this framework predicts with experiments, we performed the following simulation (based on (50), figure

bioRxiv preprint doi: https://doi.org/10.1101/804864; this version posted October 16, 2019. The copyright holder for this preprint (which was not certified by peer review) is the author/funder, who has granted bioRxiv a license to display the preprint in perpetuity. It is made available under aCC-BY-NC-ND 4.0 International license.

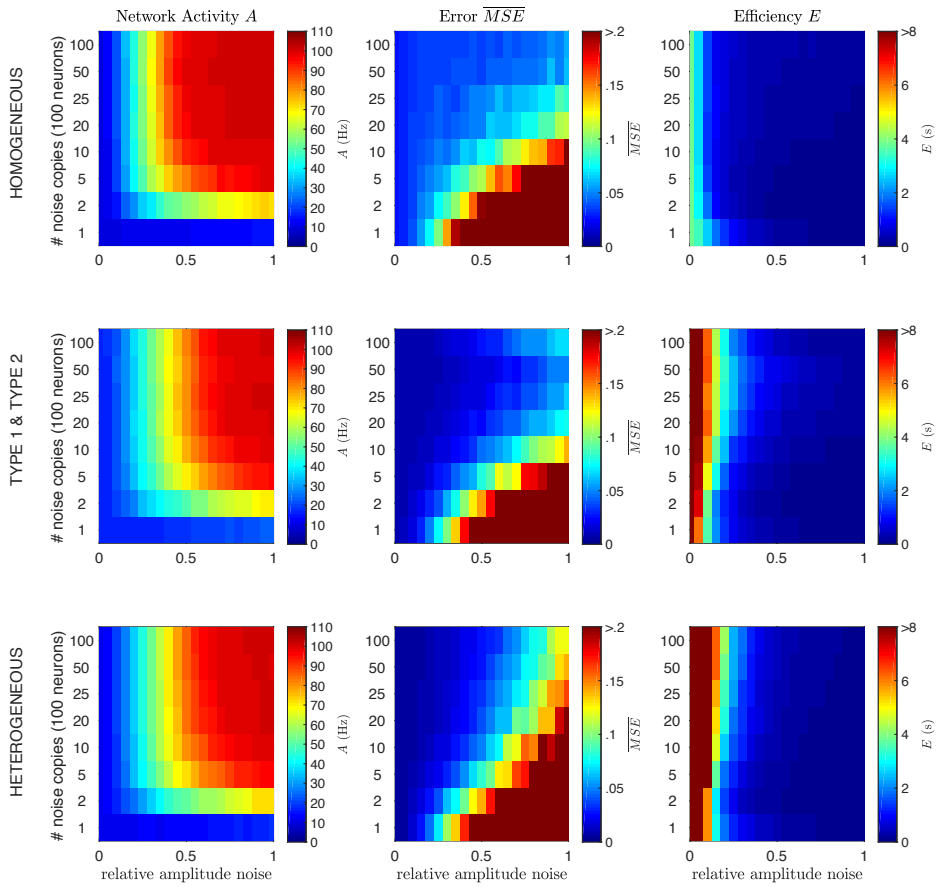

Fig. 5. Heterogeneous networks are more robust against noise. Network activity A (first column), network error $\overline{MSE}$ (second column) and efficiency E (third column) of a homogeneous network (top row), a network with 'type 1' and 'type 2' neurons (middle row) and a heterogeneous network (bottom row). Next to the stimulus, each neuron in the network was presented with a noise input, with a varying relative amplitude (horizontal axis) and number of copies of the noise signal (vertical axis; 1 copy means all neurons receive the same noise, 100 copies means all neurons receive independent noise). Network: $\Delta = 7,5$ ms, $\nu = \mu = 1,5$, $N = 100$. Stimulus: amplitude $= 10$, $\tau = 15$ ms. Noise: $\tau = 15$ ms.

6): we chose a 20 s. stimulus (exponentially filtered noise, $\tau = 15$ ms), and showed a network of $N = 100$ neurons 300 repetitions. We chose the stimulus amplitude so that the network response was around 8 Hz. In order to be able to compare neurons with similar filters and neurons with different filters, we used the 'type 1 & type 2' network (see section). To assess the effects of shared noise, each neuron received a noise signal that was the sum of an independent noise signal, and a noise signal that was shared between 10 neurons (amplitude signal = 2.7, amplitude independent noise = 0.5, amplitude correlated noise = 0.5). In this simulation, we can compare neurons that share a noise source, and neurons that don't.

In figure 6, the signal and noise correlations between 'type 1' and 'type 2' and 'on' and 'off' cells (see section and figure 3) are shown. We ran a simulation consisting of 300 trials, in which the same signal, but a different noise realization was used. We used the same method as (48)[2]:

- For the **signal correlations** (figure 6, first column), we calculated the average spike train over the 300 trials and calculated the cross-correllogram, normalized to the total average number of spikes.
- For the **noise correlations** (figure 6, second column), we subtracted the cross-correlogram of the averaged spike trains (see above) from the cross-correlograms averaged over all trials.
- For the **noise correlations, shared noise** condition (figure 6, third column), we simply calculated the noise correlations as above for two neurons that shared a noise source.

We performed this correlation analysis for two 'type 1' neurons (figure 6, top row, blue), for two 'type 2' neurons (figure 6, middle row, red) and for a 'type 1' and a 'type 2' neuron (figure 6, bottom row, purple). We performed the correlation analysis also between two neurons with the same representing filter (solid line) and with a neuron and a neuron with an inverted representing filters ('off-cells', dashed lines).

We start by looking at cells with similar filtering properties. In figure 6 A, we show that 'type 1' neurons show positive signal correlations with other 'type 1' neurons

[2]Note that the spike-count correlation is proportional to the area under the noise cross-correlogram in this method

bioRxiv preprint doi: https://doi.org/10.1101/804864; this version posted October 16, 2019. The copyright holder for this preprint (which was not certified by peer review) is the author/funder, who has granted bioRxiv a license to display the preprint in perpetuity. It is made available under aCC-BY-NC-ND 4.0 International license.

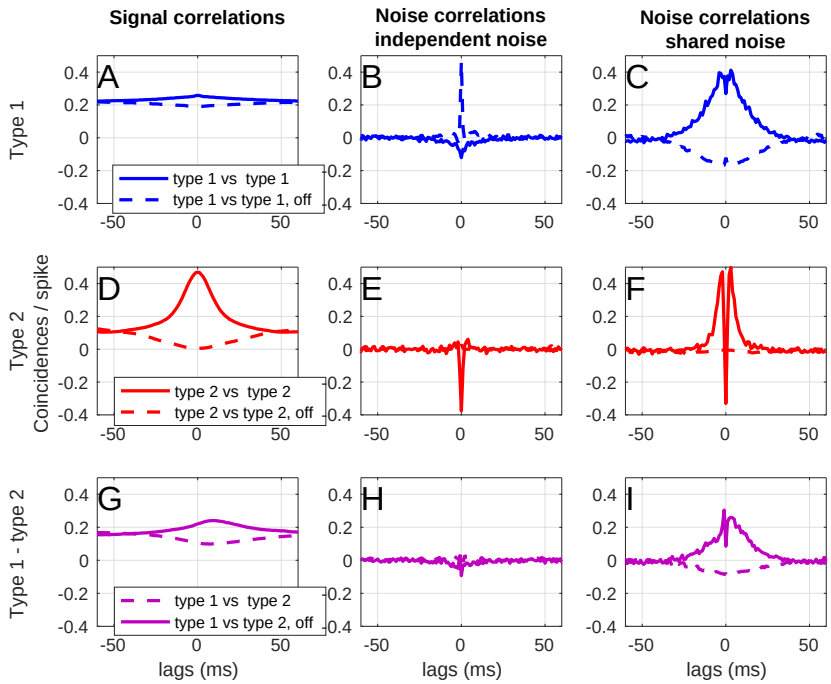

Fig. 6. Signal and noise correlations in a network with 'type 1' and 'type 2' neurons (see section and figure 3). Next to the stimulus, each neuron in the network was presented with a noise input (of which half the power was independent, and half was shared with a subset of other neurons). A) Signal correlations between 'type 1' on-cells (solid blue line) and between a 'type 1' on and off cell (dashed blue line). B) Noise correlations between 'type 1' on-cells (solid blue line) and between a 'type 1' on and off cell (dashed blue line) receiving independent noise. C) Noise correlations between 'type 1' on-cells (solid blue line) and between a 'type 1' on and off cell (dashed blue line) receiving shared noise. D) Signal correlations between 'type 2' on-cells (solid red line) and between a 'type 2' on and off cell (dashed red line). E) Noise correlations between 'type 2' on-cells (solid blue line) and between a 'type 2' on and off cell (dashed red line) receiving independent noise. F) Noise correlations between 'type 2' on-cells (solid red line) and between a 'type 2' on and off cell (dashed red line) receiving shared noise. D) Signal correlations between a 'type 1' and a 'type 2' on-cell (solid purple line) and between a 'type 1' on and a 'type 2' off cell (dashed purple line). E) Noise correlations between a 'type 1' on-cell and a 'type 2' on-cell (solid purple line) and between a 'type 1' on and a 'type 2' off cell (dashed purple line) receiving independent noise. F) Noise correlations between a 'type 1' on-cell and a 'type 2' on-cell (solid purple line) and between a 'type 1' on and a 'type 2' off cell (dashed purple line) receiving shared noise. Network parameters: $\Delta = 7,5$ ms, $\nu = \mu = 1,5$, $N = 100$, $N_{\text{trial}} = 300$. Stimulus: $\tau = 15$ ms, amplitude = 2.7. Noise: $\tau = 15$ ms, amplitude independent noise = 0.5, amplitude shared noise = 0.5.

(solid blue line), and negative signal correlations with their off-cells (dashed blue line). As expected, 'type 1'-neurons show negative noise correlations with other 'type 1'-neurons (figure 6 B, solid blue line), and positive noise correlations with their off-cells as long as noise is independent (dashed blue line). When neurons share a noise source (figure 6 C), the noise correlations are positive, but show a small negative deflection around zero lag for on cells (solid blue line). For 'type 2' neurons, we can show similar conclusions: two on-cells have positive signal correlations (figure 6 D, solid red line), negative noise correlations for independent noise ((figure 6 E, solid red line), and positive noise correlations with a negative peak around zero for shared noise ((figure 6 F, solid red line). An on and an off cell show negative signal correlations (figure 6 D, dashed red line), but hardly any noise correlations for independent noise (figure 6 E, dashed red line) or shared noise (figure 6 F, dashed red line).

We now focus at cells with different filtering properties. 'Type 1' and 'type 2' on cells show positive signal correlations (figure 6 G), solid purple line). Note that the peak is shifted towards positive lags, meaning that the 'type 2' neurons spike earlier in time than 'type 1' neurons. 'Type 1' and 'type 2' on cells show only small noise correlations for independent noise (figure 6 H, solid purple line). When noise is shared (figure 6 I, solid purple line), a small deflection at zero lag can be seen.

Under experimental conditions, correlations are often summed over a window of about 10 miliseconds or more. Therefore, we conclude that even though the predictive coding framework predicts negative noise correlations between similarly tuned neurons, and positive noise correlations between oppositly tuned neurons, these would be very hard to observe experimentally. For shared noise, we expect to see noise correlations with a similar sign as the signal correlations, but with small deflections at small lags, as shown in figure 6 C, F, I.

'Type 2' neurons show more coherence with network activity. To examine how the two different neuron types couple to the network activity in response to a temporally fluctuating stimulus, we study the spike coherence with a simulated Local Field Potential (LFP). In figure 7, we analyse the network activity of the different types of neurons, using the 'type 1 & type 2'-network (see section and figure 3). Next to the stimulus, each neuron in the network was presented with a noise input (of which half the power was independent, and half was shared with a subset of other neurons). Network: $\Delta = 7,5$ ms, $\nu = \mu = 1,5$, $N = 100$. Stimulus: $\tau = 15$ ms,

bioRxiv preprint doi: https://doi.org/10.1101/804864; this version posted October 16, 2019. The copyright holder for this preprint (which was not certified by peer review) is the author/funder, who has granted bioRxiv a license to display the preprint in perpetuity. It is made available under aCC-BY-NC-ND 4.0 International license.

amplitude = 2.7. Noise: $\tau = 15$ ms, amplitude independent noise = 0.5, amplitude shared noise = 0.5. For the network activity, each spike was convolved with a Gaussian kernel ($\sigma = 6$ ms). Looking at the network activity (figure 7 A and B), it is clear that 'type 2' neurons (red line) respond in a much more synchronized manner (high peaks), and 'type 1' neurons (blue line) respond in a much more continuous way. We quantified this, by convolving each spike with a Gaussian kernel ($\sigma = 6$ ms), and calculating both the correlations between the network activity and that of a single neuron (figure 7 C), and by calculating the 'spike-triggered network activity' (52) (figure 7 D). From this it is clear, that 'type 2' neurons show a much stronger coupling to the overall network activity (making them 'chorists') than 'type 1' neurons (making them 'soloists'). So we predict that 'type 2' neurons are more coherent with the network activity/LFP than 'type 1' neurons.

Discussion

Biological data often show a strong heterogeneity: neural properties vary considerably from neuron to neuron, even in neurons from the same network (1–5), but also see (53). Theoretical networks, however, often use a single or only a very limited amount of 'cell types', where neurons from the same cell type have the same response properties. In order to investigate the effects of network heterogeneity on neural coding, we derive a filter network that efficiently represents its input from first principles. We start with the decoding instead of with the encoding (this is not common, but has been done before (54)), and formulate a spike rule in which a neuron only fires a spike if this reduces the mean-squared error between the received input and a prediction of the input based on the output spike trains of the network, implementing a form of Lewicki's 'matching pursuit' (55). Linear decoding requires recurrent connectivity, as neurons representing different features in the input should inhibit one another to alllow linear decoding, something that has been shown in experiments (56). A similar framework has been formulated in homogeneous networks with integrate-and-fire neurons (57–60) and in networks using conductance-based models (61). Effectively, this network performs a form of coordinate transformation (62): each neuron represents a particular feature of the input, and only by combining these features the complete stimulus can be reconstructed. This network is related to autoencoders, in that it finds a sparse distributed representation of a stimulus by using an overcomplete set of basis functions in the form of a feed-forward neural-network. The homogeneous integrate-and-fire networks in this framework have been shown to operate in a tightly balanced excitatory-inhibitory regime, where a large trial-to-trial variability coexists with a maximally efficient code (63).

With the derived filter network, we are able to study both single neuron and network properties. On the single neuron level, we find that the single-neuron response properties are equivalent to those of 'type 1' and 'type 2' neurons (for an overview see (8, 9, 64)): Neurons using unimodal representing filters showed the same behaviour as 'type 1' cells (continuous input-frequency curve (6), unimodal Phase-Response Curve (PRC) (7, 65) and a unimodal Spike-Triggered Average (STA) (66)), whereas neurons using bimodal filters correspond to 'type 2' cells (discontinuous input-frequency curve, bimodal PRC and a bimodal STA). This should be the case, as the STA is a result of the filtering properties of the neuron, and proportional to the derivative of the PRC (67). In this framework, neurons with bimodal representing filters will also send bimodal Post-Synaptic Potentials (PSPs) to other neurons, so EPSPs with an undershoot or IPSPs with a depolarizing part. This might sound counterintuitive, because we often think of excitatory post-synaptic potentials (EPSP) as having a purely depolarizing effect on the membrane potential of the post-synaptic neuron, and of inhibitory post-synaptic potentials (IPSP) as having a purely hyperpolarizing effect. However, a post-synaptic potential might have both excitatory and inhibitory parts, depending on the type of synapse and the ion channels present in the membrane. For instance, an undershoot after an EPSP can be observed as an effect of slow potassium channels (17) such as I_M (16), I_A (15) or I_{AHP} (68). IPSPs can have direct depolarizing effects when the inhibition is shunting (69), (70), or due to for instance deinactivation of sodium channels, or slow activation of other depolarizing channels such as I_h. The observation that neurons using unimodal representing filters show 'type 1' behaviour and neurons using bimodal representing filters show 'type 1' behaviour gives a functional interpretation of these classical neuron types: 'type 1' cells are more efficient at representing slowly fluctuating inputs, whereas 'type 2' cells are made for representing transients and fast-fluctuating input. This can also be observed in the network activity: 'type 2' neurons show a much stronger coupling to the overall network activity (making them 'chorists' (52)) than 'type 1' neurons (making them 'soloists'). This is expected, as 'type 1' neurons are generally harder to entrain (65), whereas 'type 2' neurons generally show resonant properties (71). So we predict that 'type 2' neurons are more coherent with the network activity (local field potential) than 'type 1' neurons.

We compare both the functional coding properties and the activity of networks with different degrees of heterogeneity. We found that all networks in this framework can respond efficiently and robustly to a large variety of inputs (varying amplitude and fluctuation speed) corrupted with noise with different properties (ampitude, fluctuation speed, correlation between neurons). All networks show a high trial-to-trial variability, that decreases with the network efficiency. So we confirmed that trial-to-trial variability is not necessarily a result of noise, but is actually a hallmark of efficient coding (72–74). In-vivo recordings typically show strong trial-to-trial variability between spike trains from the same neuron, and spike trains from individual neurons are quite irregular, appearing as if a Poisson process has generated them. In in-vitro recordings on the contrary, neurons show

bioRxiv preprint doi: https://doi.org/10.1101/804864; this version posted October 16, 2019. The copyright holder for this preprint (which was not certified by peer review) is the author/funder, who has granted bioRxiv a license to display the preprint in perpetuity. It is made available under aCC-BY-NC-ND 4.0 International license.

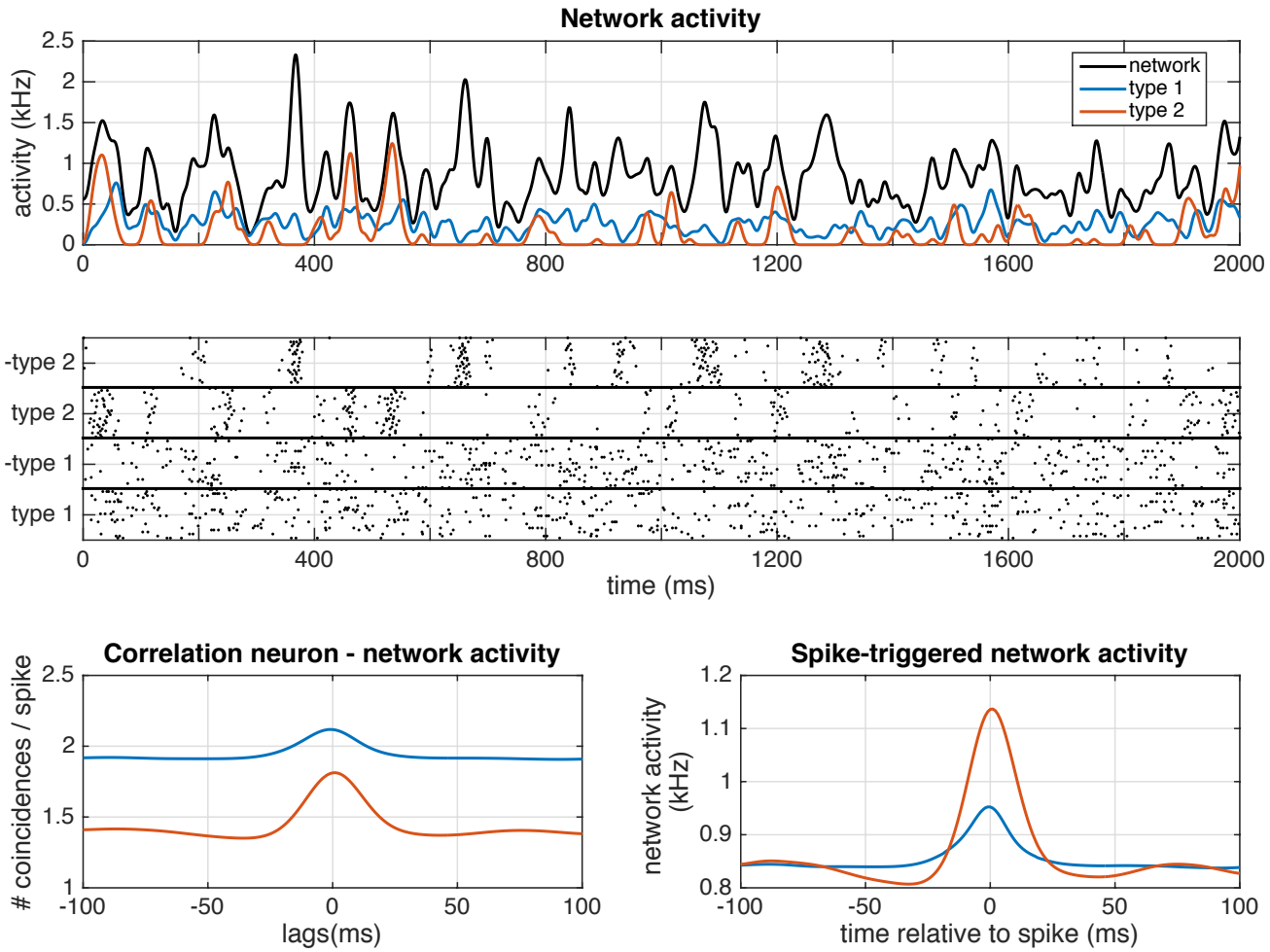

Fig. 7. Network activity in a 'type 1 & type 2' network (see section and figure 3). A) Average activity of the whole network (black), 'type 1 on cells' (blue line) and 'type 2 on cells' (red line). B) Spike response of the network. C) Average cross-correllogram between the network activity and 'type 1, on' cells (blue line) or 'type 2, on' cells (red line). D) Spike-triggered network activity for 'type 1, on' cells (blue line) or 'type 2, on' cells (red line). Next to the stimulus, each neuron in the network was presented with a noise input (of which half the power was independent, and half was shared with a subset of other neurons). Network: $\Delta = 7,5$ ms, $\nu = \mu = 1,5$, $N = 100$. Stimulus: $\tau = 15$ ms, amplitude = 2.7. Noise: $\tau = 15$ ms, amplitude independent noise = 0.5, amplitude shared noise = 0.5. For the network activity, each spike was convolved with a Gaussian kernel ($\sigma = 6$ ms)

very regular responses to injected input current, especially if this current is fluctuating ((75, 76). It is often argued that this is due to noise in the system and therefore that the relevant decoding parameter should be the firing rate over a certain time window (as opposed the timing of individual spikes, (77), but see also (78)). Here, we show in noiseless in-vivo-like simulations that the generated spike trains are irregular and show large trial-to-trial variability, even though the precise timing of each spike matters: shifting spike times decreases the performance of the network. Therefore, this model shows how the intuitively contradictory properties of trial-to-trial variability and coding with precise spike times can be combined in a single framework. Trial-t- trial variability is here a sign of degeneracy in the code: the relation between the network size, filter size and homogeneity of the network versus the amplitude determines whether there is strong or almost no trial-to-trial variability. Moreover, we show that the trial-to-trial variability and the coding efficiency depend on the frequency content of the input, as has been shown in several systems (39, 42, 44, 75).

Heterogeneous networks are more efficient than homogeneous networks, especially in representing fast-fluctuating stimuli: heterogeneous networks represent the input with a smaller error and using fewer spikes, in line with earlier research that found that heterogeneity increases the computational power of a network (23, 24) especially if they match the stimulus statistics (79). Heterogeneous networks are not only more efficient, they are also more robust against correlated noise (noise that is shared between neurons) than homogeneous networks, in line with previous results (25, 80, 81). This might be the result of heterogeneous networks using a less degenerate code: these networks are better at whitening the noise signal, because each neuron projects the noise onto a different filter, thereby effectively decorrelating the noise. Put differently, the heterogeneous network projects the signal and noise into a higher-dimensional space (62), thereby more effectivily projecting noise and signal

bioRxiv preprint doi: https://doi.org/10.1101/804864; this version posted October 16, 2019. The copyright holder for this preprint (which was not certified by peer review) is the author/funder, who has granted bioRxiv a license to display the preprint in perpetuity. It is made available under aCC-BY-NC-ND 4.0 International license.

into different dimensions. Homogeneous networks are better at compensating for independent noise. This is probably due to a combination of two factors: 1) a homogeneous network being better at compensating for erronous spikes (a 'mistake' in the estimate is easier to compensate if the same but negative filter exist than if this doesn't exist) and 2) a homogeneous network is better at representing high-amplitude signals. The optimal mix of neuron types probably depends on the stimulus statistics and remains a topic for further study.

The predictive coding framework predicts a specific correlation structure between neurons: negative noise correlations between neurons with similar tuning, and positive noise correlations between neurons with opposite tuning. This may appear to be contradictory to earlier results (82, 83). However, as neurons with similar tuning most likely recieve inputs from common sources in previous layers, these neurons will also share noise sources, resulting in correlated noise between neurons. We showed that in this situation, the negative noise correlations are only visible as small deflections of effectively positive correlations. It has been argued that in order to code efficiently and effectively, recurrent connectivity should depend on the statistical structure of the input to the network (84) and that noise correlations should be approximately proportional to the product of the derivatives of the tuning curves (85), although these authors also concluded that these correlations are difficult to measure experimentally. Others suggest that neurons might be actively decorrelated to overcome shared noise (86). We conclude that even though different (optimal) coding frameworks make predictions about correlation structures between neurons, the opposite is not true: a single correlation structure can correspondd to different coding frameworks. So measuring correlations is not sufficient (although informative) to determine what coding framework is used by a network (35, 87, 88).

ACKNOWLEDGEMENTS
FZ acknowledges support from the Netherlands Organisation for Scientific Research (Nederlandse Organisatie voor Wetenschappelijk Onderzoek, NWO) Veni grant (863.150.25) and the Radboud University (Christine Mohrmann Foundation), SD acknowledges support from Neuropole Region Île de France (NERF) and ERC consolidator grant "predispike" and BG acknowledges partial support from INSERM, CNRS, and from IDEX ANR-10-IDEX-0001-02 PSL* as well as from HSE Basic Research Program and the Russian Academic Excellence Project "5-100".

Bibliography

1. Alain Destexhe and Eve Marder. Plasticity in single neuron and circuit computations. *Nature*, 431:789–795, 2004.
2. Eve Marder and Adam L Taylor. Multiple models to capture the variability in biological neurons and networks. *Nature neuroscience*, 14(2):133–8, feb 2011. ISSN 1546-1726. doi: 10.1038/nn.2735.
3. Krishnan Padmanabhan and Nathaniel N Urban. Intrinsic biophysical diversity decorrelates neuronal firing while increasing information content. *Nature neuroscience*, 13(10):1276–82, oct 2010. ISSN 1546-1726. doi: 10.1038/nn.2630.
4. Shreejoy J Tripathy, Krishnan Padmanabhan, Richard C Gerkin, and Nathaniel N Urban. Intermediate intrinsic diversity enhances neural population coding. *Proceedings of the National Academy of Sciences*, 110(20):8248–53, may 2013. ISSN 1091-6490. doi: 10.1073/pnas.1221214110.
5. Nathan W. Gouwens, Staci A Sorensen, Jim Berg, Changkyu Lee, Tim Jarsky, Jonathan Ting, Susan M Sunkin, David Feng, Costas A Anastassiou, Eliza Barkan, Kris Bickley, Nicole Blesie, Thomas Braun, Krissy Brouner, Agata Budzillo, Shiella Caldejon, Tamara Casper, Dan Casteli, Peter Chong, Kirsten Crichton, Christine Cuhaciyan, Tanya L Daigle, Rachel Dalley, Nick Dee, Tsega Desta, Samuel Dingman, Alyse Doperalski, Nadezhda Dotson, Tom Egdorf, Michael Fisher, Rebecca A De Frates, Emma Garren, Marissa Garwood, Amanda Gary, Nathalie Gaudreault, Keith Godfrey, Melissa Gorham, Hong Gu, Caroline Habel, Kristen Hadley, James Harrington, Julie A Harris, Alex Henry, DiJon Hill, Sam Josephsen, Sara Kebede, Lisa Kim, Matthew Kroll, Tracy Lemon, Xiaoxiao Liu, Brian Long, Rusty Mann, Medea Mcgraw, Stefan Mihalas, Gabe J Murphy, Lydia Lindsay Ng, Kiet Ngo, Thuc Nghi Nguyen, Philip R Nicovich, Daniel Park, Sheana Parry, Jed Perkins, Lydia Potekhina, David Reid, Miranda Robertson, David Sandman, Martin Schroedter, Cliff Slaughterbeck, Gilberto Soler-llavina, Josef Sulc, Dan Castelli, Song-Lin Ding, Rebecca A de Frates, Brian Lee, Katherine E Link, Alice Mukora, Aaron Oldre, Aaron Szafer, Bosiljka Tasic, Naz Taskin, Corinne Teeter, Nivretta Thatra, Herman Tung, Wayne Wakeman, Grace Williams, Rob Young, Zhi Zhou, Colin Farrell, Hanchuan Peng, Michael J Hawrylycz, Ed Lein, Anton Arkhipov, Amy Bernard, John W Phillips, Hongkui Zeng, and Christof Koch. Classification of electrophysiological and morphological neuron types in the mouse visual cortex. *Nature Neuroscience*, 2019. ISSN 1546-1726. doi: 10.1038/s41593-019-0417-0.
6. A L Hodgkin. The local electric changes associated with repetitive action in a non-medullated axon. *The Journal of Physiology*, 107:165–181, 1948.
7. David Hansel, G Mato, and C Meunier. Synchrony in excitatory neural networks. *Neural computation*, 7(2):307–337, 1995. ISSN 0899-7667. doi: 10.1162/neco.1995.7.2.307.
8. John Rinzel and G Bard Ermentrout. Analysis of neural excitability and oscillations. In C Koch and I Segev, editors, *Methods in Neural Modeling: from synapses to networks*, pages 251–292. MIT Press, Cambridge, Massachusets, 1989. ISBN 0-262-11133-0.
9. Eugene M. Izhikevich. Neural Excitability, Spiking and Bursting. *International Journal of Bifurcation and Chaos in Applied Sciences and Engineering*, 10(6):1171–1266, 2000.
10. Steven A. Prescott, Y De Koninck, and Terrence J. Sejnowski. Biophysical Basis for Three Distinct Dynamical Mechanisms of Action Potential Initiation. *PLoS Computational Biology*, 4(10):e1000198, 2008.
11. Christian K. Machens, Ranulfo Romo, and Carlos D Brody. Functional, but not anatomical, separation of "what" and "when" in prefrontal cortex. *The Journal of Neuroscience*, 30(1): 350–360, 2010. ISSN 0270-6474. doi: 10.1523/JNEUROSCI.3276-09.2010.
12. M. Hausser. Diversity and Dynamics of Dendritic Signaling. *Science*, 290(5492):739–744, oct 2000. ISSN 00368075. doi: 10.1126/science.290.5492.739.
13. Istvan Mody and Robert a Pearce. Diversity of inhibitory neurotransmission through GABA(A) receptors. *Trends in neurosciences*, 27(9):569–75, sep 2004. ISSN 0166-2236. doi: 10.1016/j.tins.2004.07.002.
14. R Miles, K Toth, A I Gulyas, Norbert Hajos, and Tamás F Freund. Differences between somatic and dendritic inhibition in the hippocampus. *Neuron*, 16(4):815–823, 1996.
15. By J D Clements, P G Nelson, and S J Redman. Intracellular tetraethylammonium ions enhance group Ia excitatory post-synaptic potentials evoked in cat motoneurones. *The Journal of Physiology*, 377:267–282, 1986.
16. T. Tosaka, J. Tasaka, T. Miyazaki, and B. Libet. Hyperpolarization following activation of K+ channels by excitatory postsynaptic potentials. *Nature*, 305(8):148–150, 1983.
17. R Miles and R K S Wong. Excitatory synaptic interactions between CA3 neurones in the guinea-pig hippocampus. *The Journal of Physiology*, 373:397–418, 1986.
18. W. Hevers and H. Lüddens. The diversity of GABAA receptors. Pharmacological and electrophysiological properties of GABAA channel subtypes. *Molecular neurobiology*, 18(1): 35–86, 1998. ISSN 0893-7648. doi: 10.1007/BF02741459.
19. Daniel J Amit and Nicolas Brunel. Model of Global Spontaneous Activity and Local Structured Activity During Delay Periods in the Cerebral Cortex. *Cerebral Cortex*, 7(3):237–252, 1997.
20. Nicolas Brunel. Dynamics of Sparsely Connected Networks of Excitatory and Inhibitory Spiking Neurons. *Journal of Computational Neuroscience*, 8(183-208), 2000.
21. Carl van Vreeswijk and Haim Sompolinsky. Chaos in neuronal networks with balanced excitatory and inhibitory activity. *Science*, 274:1724–1726, 1996.
22. Carl van Vreeswijk and Haim Sompolinsky. Chaotic Balanced State in a Model Of Cortical Circuits. *Neural Computation*, 10:1321–1371, 1998.
23. Eric Hunsberger, Matthew Scott, and Chris Eliasmith. The competing benefits of noise and heterogeneity in neural coding. *Neural computation*, 26(8):1600–23, aug 2014. ISSN 1530-888X. doi: 10.1162/NECO_a_00621.
24. Renato Duarte and Abigail Morrison. Leveraging heterogeneity for neural computation with fading memory in layer 2/3 cortical microcircuits. *PLoS computational biology*, 15(4): e1006781, 2019. ISSN 15537358. doi: 10.1371/journal.pcbi.1006781.
25. Alexander S. Ecker, Philipp Berens, Andreas S Tolias, and Matthias Bethge. The effect of noise correlations in populations of diversely tuned neurons. *The Journal of Neuroscience*, 31(40):14272–83, oct 2011. ISSN 1529-2401. doi: 10.1523/JNEUROSCI.2539-11.2011.
26. E. J. Chichilnisky. A simple white noise analysis of neuronal light. *Network: Computation in Neural Systems*, 12:199–213, 2001.
27. Eero P Simoncelli, Liam Paninski, Jonathan W Pillow, and O Schwartz. Characterization of Neural Responses with Stochastic Stimuli. In M Gazzaniga, editor, *The Cognitive Neurosciences*, page 1385. MIT Press, 2004. ISBN 0262072548, 9780262072540.
28. Liam Paninski. Maximum likelihood estimation of cascade point-process neural encoding models. *Network: Computation in Neural Systems*, 15(4):243–262, nov 2004. ISSN 0954-898X. doi: 10.1088/0954-898X/15/4/002.
29. Jonathan W Pillow, Jonathon Shlens, Liam Paninski, Alexander Sher, Alan M. Litke, E. J. Chichilnisky, and Eero P Simoncelli. Spatio-temporal correlations and visual signalling in a complete neuronal population. *Nature*, 454(7207):995–9, aug 2008. ISSN 1476-4687. doi: 10.1038/nature07140.
30. Jonathan W Pillow. Likelihood-Based Approaches to Modeling the Neural Code. In K Doya, I. Ishii, A. Pouget, and R P N Rao, editors, *Bayesian Brain: Probabilistic Approaches to Neural Coding*, volume 70, chapter 3, pages 53–70. MIT Press, Cambridge, Massachusets, 2007.
31. O Schwartz, Jonathan W Pillow, N C Rust, and Eero P Simoncelli. Spike-triggered neural characterization. *Journal of Vision*, 6(4):484–507, 2006.
32. Liam Paninski, Jonathan W Pillow, and Eero P Simoncelli. Maximum likelihood estimation of a stochastic integrate-and-fire neural encoding model. *Neural Computation*, 16(12):2533–61, dec 2004. ISSN 0899-7667. doi: 10.1162/0899766042321797.

bioRxiv preprint doi: https://doi.org/10.1101/804864; this version posted October 16, 2019. The copyright holder for this preprint (which was not certified by peer review) is the author/funder, who has granted bioRxiv a license to display the preprint in perpetuity. It is made available under aCC-BY-NC-ND 4.0 International license.

33. N Brenner, S P Strong, R Koberle, William Bialek, and Rob R de Ruyter van Steveninck. Synergy in a Neural Code. *Neural Computation*, 12(7):1531–1552, 2000.
34. Eugene M. Izhikevich. Resonate-and-fire neurons. *Neural Networks*, 14(6-7):883–94, 2001. ISSN 0893-6080.
35. Bruno B Averbeck, Peter E Latham, and Alexandre Pouget. Neural correlations, population coding and computation. *Nature reviews. Neuroscience*, 7(5):358–66, may 2006. ISSN 1471-003X. doi: 10.1038/nrn1888.
36. Ho Ko, Lee Cossell, Chiara Baragli, Jan Antolik, Claudia Clopath, Sonja B. Hofer, and Thomas D. Mrsic-Flogel. The emergence of functional microcircuits in visual cortex. *Nature*, 496(7443):96–100, apr 2013. ISSN 1476-4687. doi: 10.1038/nature12015.
37. Werner M. Kistler, Wulfram Gerstner, and J L van Hemmen. Reduction of the Hodgkin-Huxley Equations to a Single-Variable Threshold Model. *Neural Computation*, 9:1015–1045, 1997.
38. Renaud Jolivet, Alexander Rauch, Hans-Rudolf Lüscher, and Wulfram Gerstner. Predicting spike timing of neocortical pyramidal neurons by simple threshold models. *Journal of Computational Neuroscience*, 21:35–49, 2006.
39. Haishan Yao, Lei Shi, Feng Han, Hongfeng Gao, and Yang Dan. Rapid learning in cortical coding of visual scenes. *Nature neuroscience*, 10(6):772–8, jun 2007. ISSN 1097-6256. doi: 10.1038/nn1895.
40. Rajeev V. Rikhye and Mriganka Sur. Spatial correlations in natural scenes modulate response reliability in mouse visual cortex. *Journal of Neuroscience*, 35(43):14661–14680, 2015. ISSN 15292401. doi: 10.1523/JNEUROSCI.1660-15.2015.
41. Uri Hasson, Rafael Malach, and David J. Heeger. Reliability of cortical activity during natural stimulation. *Trends in Cognitive Sciences*, 14(1):40–48, 2010. ISSN 13646613. doi: 10.1016/j.tics.2009.10.011.
42. Fred Rieke, D a Bodnar, and William Bialek. Naturalistic stimuli increase the rate and efficiency of information transmission by primary auditory afferents. *Proceedings of the Royal Society of London. Series B*, 262(1365):259–65, dec 1995. ISSN 0962-8452. doi: 10.1098/rspb.1995.0204.
43. Yang Dan, J J Atick, and R C Reid. Efficient coding of natural scenes in the lateral geniculate nucleus: experimental test of a computational theory. *The Journal of neuroscience*, 16(10): 3351–62, may 1996. ISSN 0270-6474.
44. Daniel A Butts, Chong Weng, Jianzhong Jin, Chun-I I Yeh, Nicholas a Lesica, Jose-Manuel M Alonso, and Garrett B Stanley. Temporal precision in the neural code and the timescales of natural vision. *Nature*, 449(7158):92–96, sep 2007. ISSN 1476-4687. doi: 10.1038/nature06105.
45. Gaëlle Desbordes, Jianzhong Jin, Jose-Manuel Alonso, and Garrett B Stanley. Modulation of temporal precision in thalamic population responses to natural visual stimuli. *Frontiers in systems neuroscience*, 4(November):151, 2010. ISSN 1662-5137. doi: 10.3389/fnsys.2010.00151.
46. Marlene R. Cohen and William T. Newsome. Context-Dependent Changes in Functional Circuitry in Visual Area MT. *Neuron*, 60(1):162–173, 2008. ISSN 08966273. doi: 10.1016/j.neuron.2008.08.007.
47. Ehud Zohary, Michael N. Shadlen, and William T. Newsome. Correlated neuronal discharge rate and its implications for psychophysical performance. *Nature*, 370(6485):140–143, 1994. ISSN 00280836. doi: 10.1038/370140a0.
48. W Bair, E Zohary, and William T. Newsome. Correlated firing in macaque visual area MT: time scales and relationship to behavior. *The Journal of Neuroscience*, 21(5):1676–1697, 2001. ISSN 1529-2401. doi: 21/5/1676[pii].
49. Jaime de la Rocha, Brent Doiron, Eric T Shea-Brown, Kresimir Josic, and Alex D Reyes. Correlation between neural spike trains increases with firing rate. *Nature*, 448(7155):802–6, aug 2007. ISSN 1476-4687. doi: 10.1038/nature06028.
50. Gašper Tkačik, Olivier Marre, Dario Amodei, Elad Schneidman, William Bialek, and Michael J. Berry. Searching for collective behavior in a large network of sensory neurons. *PLoS computational biology*, 10(1):e1003408, jan 2014. ISSN 1553-7358. doi: 10.1371/journal.pcbi.1003408.
51. Marlene R Cohen and Adam Kohn. Measuring and interpreting neuronal correlations. *Nature neuroscience*, 14(7):811–9, jul 2011. ISSN 1546-1726. doi: 10.1038/nn.2842.
52. Michael Okun, Nicholas a. Steinmetz, Lee Cossell, M. Florencia Iacaruso, Ho Ko, Péter Barthó, Tirin Moore, Sonja B. Hofer, Thomas D. Mrsic-Flogel, Matteo Carandini, and Kenneth D. Harris. Diverse coupling of neurons to populations in sensory cortex. *Nature*, 521 (7553):511–515, 2015. ISSN 0028-0836. doi: 10.1038/nature14273.
53. Shreejoy J Tripathy, Shawn D Burton, Matthew Geramita, Richard C Gerkin, Nathaniel N Urban, and Nathaniel N Urban. Brain-wide analysis of electrophysiological diversity yields novel categorization of mammalian neuron types. *Journal of Neurophysiology*, in press, 2015. doi: 10.1152/jn.00237.2015.
54. Austin J. Brockmeier, John S Choi, Evan G Kriminger, and Joseph T Francis. Neural Decoding with Kernel-based Metric Learning. *Neural computation*, 26:1080–1107, 2014. ISSN 1530888X. doi: 10.1162/NECO.
55. Evan Smith and Michael S Lewicki. Efficient coding of time-relative structure using spikes. *Neural Computation*, 17(1):19–45, jan 2005. ISSN 0899-7667. doi: 10.1162/0899766052530839.
56. Vicente Botella-Soler, Stéphane Deny, Georg Martius, Olivier Marre, and Gašper Tkačik. Nonlinear decoding of a complex movie from the mammalian retina. *PLOS Computational Biology*, 14(5):e1006057, may 2018. ISSN 1553-7358. doi: 10.1371/journal.pcbi.1006057.
57. Martin Boerlin and Sophie Denève. Spike Based Population Coding and Working Memory. *PLoS Computational Biology*, 7(2):e1001080, 2011.
58. Martin Boerlin, Christian K. Machens, and Sophie Denève. Predictive Coding of Dynamical Variables in Balanced Spiking Networks. *PLoS Computational Biology*, 9(11), 2013. doi: 10.1371/journal.pcbi.1003258.
59. Ralph Bourdoukan, David G. T. Barrett, Christian K. Machens, and Sophie Denève. Learning optimal spike-based representations. In P. Bartlett, F.C.N. Pereira, C.J.C. Burges, L. Bottou, and K.Q. Weinberger, editors, *Advances in Neural Information Processing Systems 25*, pages 2294–2302, 2012.
60. Sophie Denève, Alireza Alemi, and Ralph Bourdoukan. The Brain as an Efficient and Robust Adaptive Learner. *Neuron*, 94(5):969–977, 2017. ISSN 10974199. doi: 10.1016/j.neuron.2017.05.016.
61. Michael A Schwemmer, Adrienne L Fairhall, Sophie Denève, and Eric T Shea-Brown. Constructing Precisely Computing Networks with Biophysical Spiking Neurons. *Journal of Neuroscience*, 35(28):10112–10134, jul 2015. ISSN 0270-6474. doi: 10.1523/JNEUROSCI.4951-14.2015.
62. Alexandre Pouget and Lawrence H. Snyder. Computational approaches to sensorimotor transformations. *Nature Neuroscience*, 3(11s):1192–1198, 2000. ISSN 15461726. doi: 10.1038/81469.
63. Sophie Denève and Christian K. Machens. Efficient codes and balanced networks. *Nature neuroscience*, 19(3):375–82, 2016. ISSN 1546-1726. doi: 10.1038/nn.4243.
64. Steven A. Prescott, Stéphanie Ratté, Y De Koninck, and Terrence J. Sejnowski. Pyramidal Neurons Switch From Integrators In Vitro to Resonators Under In Vivo-Like Conditions. *Journal of Neurophysiology*, 100:3030–3042, 2008.
65. G Bard Ermentrout. Type I Membranes, Phase Resetting Curves, and Synchrony. *Neural Computation*, 8:979–1001, 1996.
66. Boris S. Gutkin, G Bard Ermentrout, and Alex D Reyes. Phase-response curves give the responses of neurons to transient inputs. *Journal of neurophysiology*, 94(2):1623–35, aug 2005. ISSN 0022-3077. doi: 10.1152/jn.00359.2004.
67. G Bard Ermentrout, R F Galan, and Nathaniel N Urban. Relating neural dynamics to neural coding. *Physical Review Letters*, 99(24):248103, 2007.
68. R A Nicoll and B E Alger. Synaptic excitation may activate a calcium-dependent potassium conductance in hippocampal pyramidal cells. *Science*, 212(4497):957–959, 1981.
69. A T Gulledge and Greg J Stuart. Excitatory Actions of GABA in the Cortex. *Neuron*, 37: 299–309, 2003.
70. Peter Jonas and György Buzsáki. Neural Inhibition. *Scholarpedia*, 2(9):3286, 2007.
71. Eugene M. Izhikevich. *Dynamical Systems in Neuroscience: The Geometry of Excitability and Bursting*. MIT Press, Cambridge, MA, 2007. ISBN 978-0-262-09043-8.
72. Sophie Denève and Matthew Chalk. Efficiency turns the table on neural encoding, decoding and noise. *Current Opinion in Neurobiology*, 37:141–148, 2016. ISSN 18736882. doi: 10.1016/j.conb.2016.03.002.
73. Felix Franke, Michele Fiscella, Maksim Sevelev, Botond Roska, Andreas Hierlemann, and Rava Azaredo da Silveira. Structures of Neural Correlation and How They Favor Coding. *Neuron*, 89(2):409–422, 2016. ISSN 0896-6273. doi: 10.1016/j.neuron.2015.12.037.
74. Jorrit S. Montijn, Guido T. Meijer, Carien S. Lansink, and Cyriel M.A. Pennartz. Population-Level Neural Codes Are Robust to Single-Neuron Variability from a Multidimensional Coding Perspective. *Cell Reports*, pages 91–101, 2016. ISSN 22111247. doi: 10.1016/j.celrep.2016.07.065.
75. Rob R de Ruyter van Steveninck, Geoffrey D Lewen, S P Strong, R Koberle, and William Bialek. Reproducibility and Variability in Neural Spike Trains. *Science*, 275:1805–1808, 1997. doi: 10.1126/science.275.5307.1805.
76. Z F Mainen and Terrence J. Sejnowski. Reliability of Spike Timing in Neocortical Neurons. *Science*, 268:1503–1506, 1995.
77. M N Shadlen and William T. Newsome. Noise, neural codes and cortical organization. *Current Opinion in Neurobiology*, 4(4):569–79, aug 1994. ISSN 0959-4388.
78. Alfonso Renart and Christian K. Machens. Variability in neural activity and behavior. *Current Opinion in Neurobiology*, 25:211–220, 2014. ISSN 18736882. doi: 10.1016/j.conb.2014.02.013.
79. Diana E Mitchell, Annie Kwan, Jerome Carriot, Maurice J Chacron, and Kathleen E Cullen. Neuronal variability and tuning are balanced to optimize naturalistic self- motion coding in primate vestibular pathways. *eLife*, page e43019, 2018. doi: 10.7554/eLife.43019.
80. Maoz Shamir and Haim Sompolinsky. Implications of neuronal diversity on population coding. *Neural computation*, 18(8):1951–86, aug 2006. ISSN 0899-7667. doi: 10.1162/neco.2006.18.8.1951.
81. Haim Sompolinsky, Hyoungsoo Yoon, Kukjin Kang, and Maoz Shamir. Population coding in neuronal systems with correlated noise. *Physical Review E*, 64(5):051904, oct 2001. ISSN 1063-651X. doi: 10.1103/PhysRevE.64.051904.
82. Kenneth D. Harris and Thomas D. Mrsic-Flogel. Cortical connectivity and sensory coding. *Nature*, 503(7474):51–8, 2013. ISSN 1476-4687. doi: 10.1038/nature12654.
83. Ho Ko, Sonja B. Hofer, Bruno Pichler, Katherine a Buchanan, P Jesper Sjöström, and Thomas D. Mrsic-Flogel. Functional specificity of local synaptic connections in neocortical networks. *Nature*, 473(7345):87–91, 2011. ISSN 0028-0836. doi: 10.1038/nature09880.
84. Jeffrey M Beck and Alexandre Pouget. Insights from a Simple Expression for Linear Fisher Information in a Recurrently Connected Population of Spiking Neurons. *Neural Computation*, 23(6):1484–1502, 2011.
85. Rubén Moreno-Bote, Jeffrey M Beck, Ingmar Kanitscheider, Xaq Pitkow, Peter Latham, and Alexandre Pouget. Information-limiting correlations. *Nature Neuroscience*, 17(10):1410–1417, 2014. ISSN 1097-6256. doi: 10.1038/nn.3807.
86. Alexander S. Ecker, Philipp Berens, Georgios A Keliris, Matthias Bethge, Nikos K Logothetis, and Andreas S Tolias. Decorrelated Neuronal Firing in Cortical Microcircuits. *Science*, 327:584–587, 2010.
87. Gašper Tkačik, Jason S. Prentice, Vijay Balasubramanian, and Elad Schneidman. Optimal population coding by noisy spiking neurons. *Proceedings of the National Academy of Sciences of the United States of America*, 107(32):14419–14424, 2010. ISSN 00278424. doi: 10.1073/pnas.1004906107.
88. Elad Schneidman. Noise, Correlations, and Information in Neural Population Codes. In Michael S. Gazzaniga and George R. Mangun, editors, *The Cognitive Neurosciences*, chapter 29, pages 319–336. MIT PRess, 5 edition, 2014. ISBN 9783540773405.
89. Peter Dayan and L. F. Abbott. *Theoretical Neuroscience: Computational and Mathematical Modeling of Neural Systems*. MIT Press, 2001. ISBN 0262041995.
90. Liam Paninski. Convergence properties of three spike-triggered analysis techniques. *Network: Computation in Neural Systems*, 14(3):437–64, aug 2003. ISSN 0954-898X.
91. Jonathan W Pillow, Liam Paninski, Valerie J Uzzell, Eero P Simoncelli, and E. J. Chichilnisky. Prediction and decoding of retinal ganglion cell responses with a probabilistic spiking model. *The Journal of Neuroscience*, 25(47):11003–13, nov 2005. ISSN 1529-2401. doi: 10.1523/JNEUROSCI.3305-05.2005.
92. Wilson Truccolo, Uri T Eden, Matthew R Fellows, John P Donoghue, and Emery N. Brown.

bioRxiv preprint doi: https://doi.org/10.1101/804864; this version posted October 16, 2019. The copyright holder for this preprint (which was not certified by peer review) is the author/funder, who has granted bioRxiv a license to display the preprint in perpetuity. It is made available under aCC-BY-NC-ND 4.0 International license.

A point process framework for relating neural spiking activity to spiking history, neural ensemble, and extrinsic covariate effects. *Journal of Neurophysiology*, 93(2):1074–89, feb 2005. ISSN 0022-3077. doi: 10.1152/jn.00697.2004.